STEREO-MAPPING OF PLANET VENUS FROM MAGELLAN SAR IMAGES: A STATUS REPORT

F. Leberl, K. Maurice
VEXCEL Corporation, Boulder, Colorado, USA 80301

ABSTRACT

We report on the current status of stereo-mapping of the surface of planet Venus from side-looking radar images created in the Magellan-mission of NASA. We find excellent vertical exaggeration that is more pronounced than in aerial photography.

Measurements appear repeatable within ± 30 m and accurate to within ± 100 m.

1. INTRODUCTION

NASA's Magellan mission to map the planet Venus is the most ambitious planetary imaging project ever. Venus has a surface equal in size to Earth, but has no oceans. Coverage of the planet's surface therefore requires three times the images one would need on Earth. At a resolution of 75 m per pixel, Magellan exceeds the resolution of the original Landsat-MSS sensor and has collected more data than all previous planetary missions combined. Table 1 summarizes key facts about Magellan. The data of interest to map the surface are:

- the synthetic aperture radar images (pixel sizes of 75 m);
- the altimetric measurements spaced at about 10 km to 20 km;
- the radiometric observations of emmissivity of the surface with pixel sizes of 25 km.

The mission offers unique challenges to radargrammetry: more than 90% of the surface have been imaged, and nearly half of the surface was imaged twice or more. No ground control exists. About 20% of the images present a same-side stereo coverage; about 45% of the surface is covered by opposite-side stereo data.

Date of launch from Kennedy Space Center, Florida	4 May 1989
Beginning of systematic radar imaging	15 September 1990
Completion of initial coverage (all 360°, Cycle 1)	15 May 1991
Completion of second coverage (Cycle 2)	14 January 1992
Orbit inclination (but images pole!)	85°
Spacecraft altitude above surface at periapsis	294 km
Spacecraft altitude above surface at apoapsis	8458 km
Radar image pixel size	75 m by 75 m
Radar image range resolution	88 m (0.59μsec)
Radar image azimuth resolution at 5 to 17 looks per pixel	120 m
Look angle off-nadir	See Figure 1
Radar wavelength	12.6 cm
Angular width of image at antenna, at periapsis and 80°N	2° and 0.5°

Table 1: Key facts about Magellan with relevance to stereo-radargrammetry.

While a considerable number of technical papers has been authored about the subject of stereo-radargrammetry, very little has been exercised on large, real-life data sets. Therefore, use of Magellan radar images to develop a detailed topographic relief requires pioneering efforts.

We report in this paper about the current state of affairs in extracting Digital Elevation Models (DEMs) from overlapping radar images of the surface of Venus. This effort is supervised by a Stereo Analysis Work Group of the NASA Mission's governing Project Science Group with the active participation of engineers and scientists at the Jet Propulsion Laboratory, US Geological Survey, VEXCEL Corporation, MIT and others.

The mission consumed in excess of $700 million to build the system, get it into orbit around Venus, and receive and store the data. This resulted in satisfying the nominal goals of the Mission, namely to develop a single image coverage of 70% of the planet. It was only in an *extended mission* that the second coverage was created that supports the stereo work, at a cost of about $45 million. In contrast, nearly no funding has become available to process the stereo images into useful DEMs.

2. DATA COVERAGE

With a planetary radius of 6,051 km, the surface of Venus covers $4.6 * 10^8$ sq. km. These are imaged into 1,650 images extending from pole to pole with 220,000 pixel along track, 350 pixels across track. These Full Resolution Basic Image Data Records (F-BIDRs) are subject to radargrammetric processing. Images are taken from an elliptical orbit from an altitude above the poles of about 2,000 km and at periapsis of about 295 km. As the side looking radar (SAR) images are being taken the sensor looked East (Cycle 1). A second coverage of the planet was taken with the sensor looking West (in Cycle 2). About 45% of the planet is covered by both East- and West- looking data. The missing 55% are a result of occasional obstacles to imaging, e.g. if the sun is behind Venus and Earth, or if the radar malfunctions.

A third coverage created images again by looking East, but at a different angle (Cycle 3). About 20% of the surface will be covered by September, 1992, with two sets of overlapping images both looking East and representing a same-side stereo data set. Given that on Earth only 1/3 of the surface is land, the Magellan stereo data cover a surface equal to 60% of the Earth's land masses.

The elliptical spacecraft orbit forced the imaging radar to look at the surface with varying angles. Over the poles the spacecraft is 2,000 km above the surface, looking down steeply at look-angles of 7° to 11° off nadir. At the 300 km perapsis, the look-angles can be kept much larger at 43° to 55°. Each imaging cycle therefore has a specific desired look angle profile (DLAP). Figure 1 presents Magellan's look angle profiles.

The ellipticity of the orbit and differences in look angles result in the fact that an individual Magellan image (an F-BIDR) traverses numerous other images from a different Cycle:

1 image of Cycle 1 East Looking (EL) can traverse more than 100 images of Cycle 2, West-looking (WL).

1 image of Cycle 1 (LL) can traverse 35 images of Cycle 3 (EL).

1 image of Cycle 2 (WL) can traverse more than 100 images of Cycle 3 (EL).
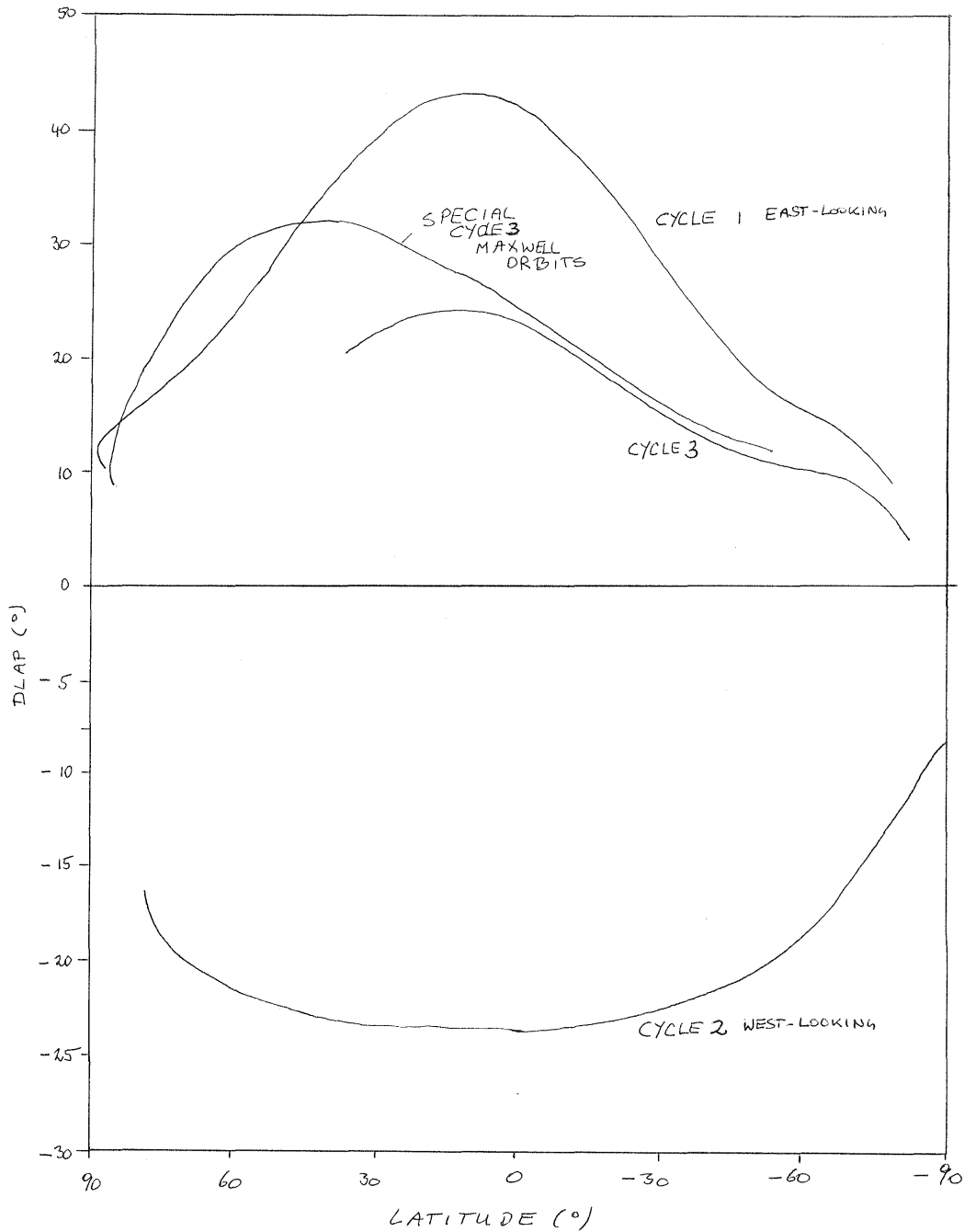
<u>Figure 1:</u> Look-angle profiles during the three initial
imaging cycles of Magellan.

This results in a need to cope with very large data sets if one
wants to process Magellan data efficiently. At the Mission's
Image Processing Laboratory, a disk farm with 190 GB is kept
on-line.

Figure 2 presents a set of radar images from each of the 3
cycles.
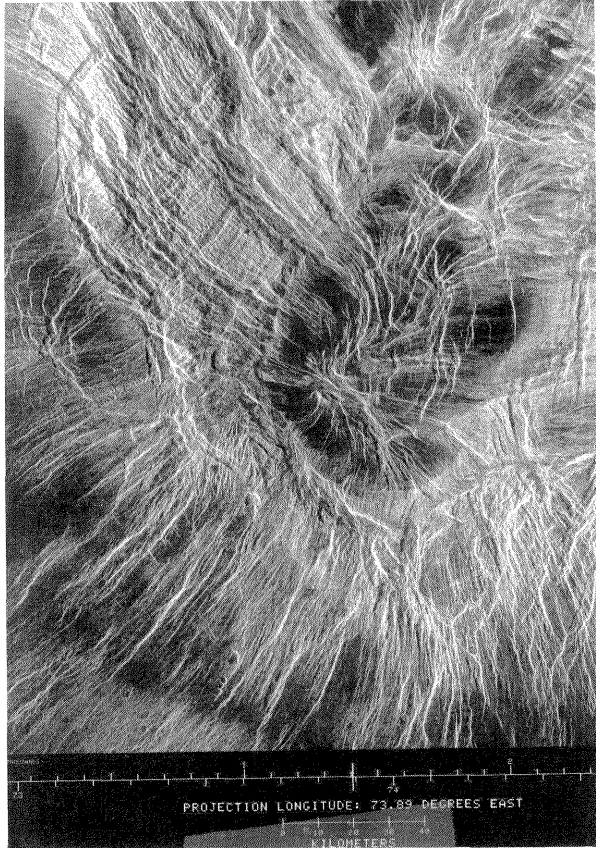
3. PROCESSING STRATEGIES

The genesis of Magellan's stereo coverage as an "after
thought", combines with the non-existence of funds to develop
and process stereo data in a systematic manner, to obstruct the
well-thought-out definition of a stereo processing strategy.
However, the basic elements of a process are obvious.
Processing *must* be automated to be feasible at all, given the
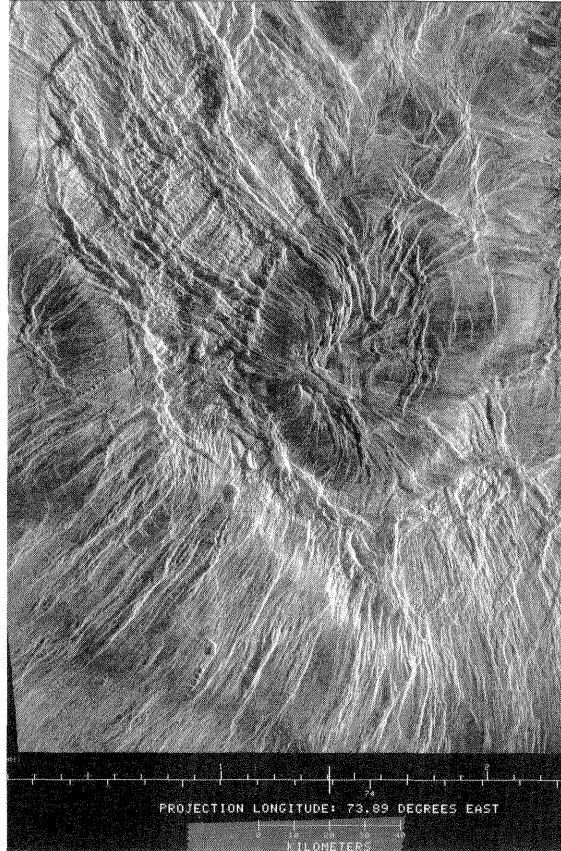monumental data quantities.

3.1 Ephemeris Adjustment

The spacecraft state and attitude vector must be known to
within a pixel or better than 75 m. This is not a trivial
accomplishment for orbits around a distant planet; it is,
however, feasible. To accomplish this goal, individual groups
of orbits are adjusted with the simultaneous use of Earth-based
Doppler observations, star-observations, use of "tie-points"
(i.e. landmarks in overlapping images) and a rigorous sensor
model. At the time of this writing, it was not clear whether tie-

CYCLE 1 E.L.

CYCLE 2 E.L.

CYCLE 2 W.L.

PROJECTION LONGITUDE: 73.89 DEGREES EAST

KILOMETERS

PROJECTION LONGITUDE: 73.89 DEGREES EAST

KILOMETERS

PROJECTION LONGITUDE: 73.68 DEGREES EAST
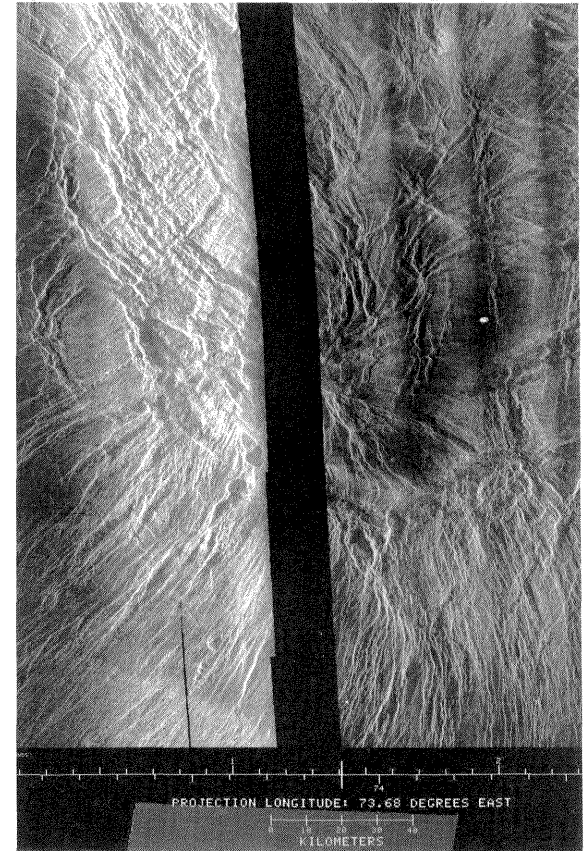
KILOMETERS

<u>Figure 2:</u> Examples of Magellan SAR images from three different look angles at an area 2° South of the equator, 74° East longitude.

points were really necessary, provided a best gravity model for the planet is available to model the orbits.

3.2 DEM Image Match Points

Image matches are obtained by normalized cross-correlation of overlapping images. While radar images may call for radar-specific radiometric and geometric features in an image matching system, such algorithms do not exist. Instead, regular cross-correlation matching is being used in initial work (Leberl et al., submitted).

3.3 Intersecting Terrain Points

A pair of image match points (x',y',x'',y'') results in a surface point XYZ based on a sensor model that converts the image measurements into a slant range and Doppler cone, and associates this with the spacecraft's state and velocity vector.

3.4 Ortho-Rectifying the Images

The x',y' and XY(Z) coordinates are the basis for ortho-rectifying the images into a planetary map coordinate system, so that an image mosaic emerges from combining individual ortho-rectified images into image map quadrangles.

3.5 Gridding the DEM

The computed mass points at their XYZ locations need to be converted into a regular grid of DEM points by an interpolation process.

3.6 Quality Assessment and Editing

Of course any extracted data need to be verified for their accuracy. There are several options:

  (a) Visual inspection and manual editing;

  (b) Figures of merit from;
       image matching;
       stereo-intersection.
  (c) Use of overlaps in stereo image pairs and
       assessment of internal consistency.

3.7 Refining the DEM with Shape-From-Shading

The topographic expression inherent in radar images has been the reason that geological users of radar-stereo DEMs have been able to manually correct DEMs: the geological expert will use geomorphological details visible to the human interpreter of the images, but this detail is not available from stereo-parallaxes.

This has been the driving force behind the development of a DEM-refinement scheme based on converting local brightness differences to local slope differences. This has shown to improve the *local* morphology of the DEM (Thomas et al., 1991). The process represents an automated DEM-editor or "air brush" to add detail on the pixel-level to a DEM that otherwise would have postings every 10 to 15 pixels.

3.8 Going From Image to DEM

The process described in subsections 3.1 to 3.7 avoids the use of a *real-time math-model* for an analytical plotter. Instead the DEM is produced as if a stereo comparator had been employed.

The on-line real-time relationship between the planetary XYZ system and image spaces x',y',x'',y'' could be desireable in an interaction with the stereo images, but is not needed in the creation of DEMs and image maps.

4. SAMPLE RESULTS

Figure 3 is the perspective view of a DEM created from the stereo pair in Figures 2a, b. At the time of this writing, an end-
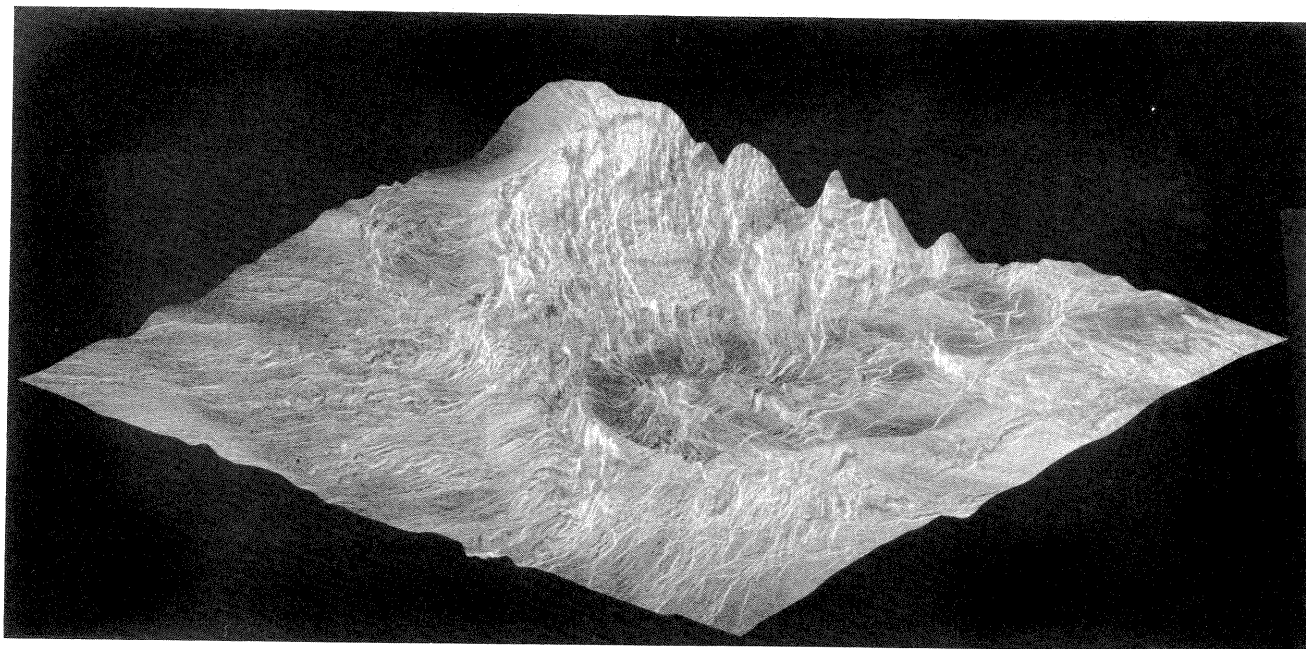

Figure 3: Perspective view of a stereo-derived DEM of 2000 x 6000 pixels covering 150 x 150 sq. km. Area covered by Figure 2. The image is draped over the DEM. Elevation differences are in the range of 2 km, and slopes of more than 30° occur.

to-end radargrammetric process as described in Section 3 was not completed. Therefore, Figure 3 is the result of an approximate procedure based on mosaicked images. Individual new basic images are projected onto a coarse topographic model from NASA's Pioneer Venus mission and a (semi-controlled) mosaic results. Overlapping mosaics provide parallax differences which represent surface shape with respect to the Pioneer-Venus topographic model (Leberl et al.; in print a, b; 1992). Errors of navigation, if present, will propagate into the mosaics and therefore lead to (false) observed parallaxes.

Figure 3 therefore is a product of uncertain absolute accuracy. However, it quantifies elevation differences and terrain slopes. We find such elevation differences to be in the amount of 2 km, and slopes of up to 34°.

5. ASSESSMENTS OF ACCURACY

5.1 Comparing Overlapping Ortho-Rectified Images

The elevation values from Figure 3 permit one to orthorectify the input image mosaics. A comparison of orthorectified mosaics results in local discrepancies of only ± 1 pixel, indicating that within the considered region the elevation differences were correct to within a fraction of a pixel. This conclusion is based on the consideration that an orthorectification is in error by a value dx, if the input elevation is in error by dh as follows:

$$dx = dh / \tan \theta$$

where θ is the incidence angle. Orthorectifying two same-side images, we find

$$dx' - dx'' = dh / \tan \theta' - dh / \tan \theta''.$$

If the discrepancy $\Delta x = dx' - dx''$ between two ortho images is 1 pixel or 75 m, then

$$75m = dh(1/\tan \theta' - 1/\tan \theta''),$$

and with $\theta' = 40°$ and $\theta'' = 20°$

$$dh = 75 \text{ m} / 1.56 = 48 \text{ m}.$$

for the case of Figure 3. Therefore, an elevation error of about 50 m will result in a discrepancy of 1 pixel between ortho-rectified stereo-images from Cycles 1 and 3.

5.2 Theoretical Assessments

A theoretical assessment of accuracy results from propagating the limited accuracy σ_r of slant ranges into an elevation uncertainty σ_h as often discussed in the literature:

$$\sigma_h \approx \frac{(\sin^2 \theta' + \sin^2 \theta'')^{1/2}}{\sin (\theta' - \theta'')} * \sigma_r$$

Independently, a parallax measurement error ddp will translate into an elevation error dh as follows:

$$dh = ddp (1/\tan \theta' - 1/\tan \theta'').$$

Figure 4 plots values for dh as a function of geographic latitude φ, which in turn defines the look angles off-nadir θ', θ'' via the DLAP-curves (see Figure 1).
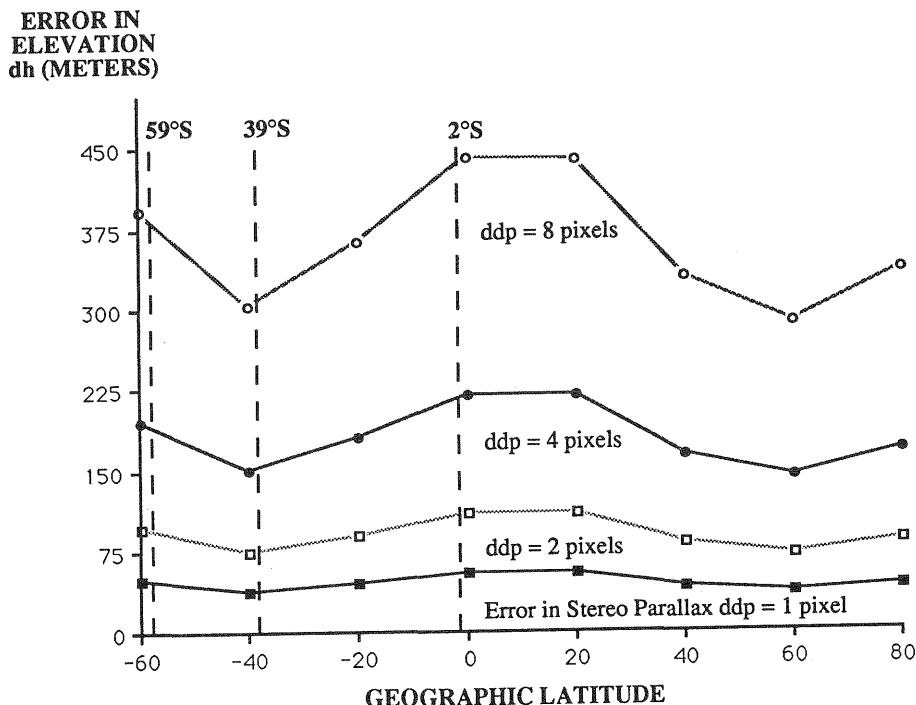

Figure 4: Theoretical accuracy prediction for elevation measurements from Magellan stereo radar images.

799

5.3 Parallax Measurements

How well can the parallax difference be measured? Experiments with visual repeat measurements provide confidence that an operator can define the stereo matches to within ±0.6 pixels. Automated matching may differ from visual observations with an r.m.s. error of ±2 pixels (Leberl et al., submitted).

5.4 Future Work

Hopes to quantitively assess Magellan-stereo accuracies are based on the analysis of internal mismatches in overlapping stereo-models at higher latitudes, on assessing elevation differences from stereo and from exploiting symmetric features in single images (Leberl et al., 1991).

5.5 Vertical Exaggeration

The parallax-to-height conversion in photogrammetry typically is by a factor of about 0.6 (the so-called base-to-height ratio). Therefore a 100 m photographic parallax will be caused by a 167 m terrain elevation difference.

In Magellan's radar stereo images, this is a ratio of 1.4 or more: a 100 m parallax will be caused by only a 60 m elevation difference. Therefore we find that Magellan stereo images can have very large stereo parallaxes. An error of parallax of 1 pixel will result in an error of elevation of only 0.6 pixels. As a result we have a surprisingly strong vertical expression in Magellan SAR stereo data, which is stronger than conventional mapping photography could produce!

6. CONCLUSION, OUTLOOK

Magellan has created the largest stereo radar data set ever. The vertical expression of relief in these stereo-models is stronger than it would be in mapping photography, and stronger than in past air or spacecraft stereo radar on Earth.

We are developing tools to process these data with rigorous radargrammetric methods based on state and velocity vectors of the spacecraft and a sensor model of the SAR. In the interim demonstration products are being generated with simplified algorithms to review the capabilities of Magellan as a stereo mapping system. We believe that accuracies of parallax measurement are about ±1 to ±2 pixels, and accuracy of terrain elevation can be in the range of ±100 m.

ACKNOWLEDGMENT

RADARGRAMMETRIC PUBLICATIONS ABOUT MAGELLAN

Leberl, F., K. Maurice, J. Thomas, M. Millot, (Submitted), *Automated Radar Image Matching Experiment.* ISPRS J. of Photogrammetry and Remote Sensing.

Leberl, F., K. Maurice, J. Thomas, W. Kober (1991) *Radargrammetric Measurements from the Initial Magellan Coverage of Planet Venus.* Photogrammetric Engineering and Remote Sensing, Vol. 57, No. 12, pp. 1561-1570.

Leberl, F., K. Maurice, J. Thomas, C. Leff, S. Wall (in print), *Images and Topographic Relief at the North Pole of Venus.* J. Geophysical Research.

Leberl, F. W., J. K. Thomas, K. E. Maurice (in print), *Initial Results From the Magellan Stereo-Experiment.* J. Geophysical Research.

Leberl, F. W., K. E. Maurice, J. K. Thomas (1992) *Radargrammetric Analysis With Magellan Data of Planet Venus.* Proc. 58th Annual Convention, American Society of Photogrammetry and Remote Sensing Conference, Albuquerque, NM, pp. 253-263.

Thomas, J., W. Kober, F. Leberl (1991) *Multiple Image SAR Shape-from-Shading.* Photogrammetric Engineering and Remote Sensing, Vol. 57, No. 1, pp. 51-59.